

# Recurrent Neural Network Training with Convex Loss and Regularization Functions by Extended Kalman Filtering

Alberto Bemporad\*

November 5, 2021

## Abstract

We investigate the use of extended Kalman filtering to train recurrent neural networks for data-driven nonlinear, possibly adaptive, model-based control design. We show that the approach can be applied to rather arbitrary convex loss functions and regularization terms on the network parameters. We show that the learning method outperforms stochastic gradient descent in a nonlinear system identification benchmark and in training a linear system with binary outputs. We also explore the use of the algorithm in data-driven nonlinear model predictive control and its relation with disturbance models for offset-free tracking.

**Keywords:** Recurrent neural networks, nonlinear system identification, extended Kalman filtering, nonlinear model predictive control.

## 1 Introduction

The use of artificial neural networks (NNs) for control-oriented modeling of dynamical systems, already popular in the nineties [1], is flourishing again thanks to the wide success of machine learning in many application domains and to the availability of excellent software libraries for training NN models. Most frequently, *feedforward* NNs are used for modeling the output function in a neural-network autoregressive model with exogenous inputs (NNARX). On the other hand, *recurrent* neural networks (RNNs), as they are state-space models, are often more adequate for capturing the behavior of dynamical systems in a compact way. However, contrarily to training NNARX models based on minimizing the one-step-ahead output prediction error, training RNNs is more difficult due to the presence of the hidden states of the network. To circumvent this issue, procedures for learning neural state-space models were proposed in [2, 3], based on the idea of finding a (reduced-order) state-space realization of a NNARX model during training and considering the values of a (thin) inner layer of the model as the state vector.

To avoid unrolling the open-loop prediction of an RNN over the entire training dataset, sub-optimal approaches were proposed, such as truncated backpropagation through time (TBPTT) [4]. Motivated by the fact that a similar issue of recurrence occurs in minimizing the *simulation* error when training NNARX models, the authors in [5] proposed to learn RNNs based on splitting the dataset into smaller batches and penalizing the inconsistency between state predictions across consecutive batches. Due to the difficulty of computing gradients of full unrolls and/or the presence

---

\*The author is with the IMT School for Advanced Studies, Piazza San Francesco 19, Lucca, Italy. Email: [alberto.bemporad@imtlucca.it](mailto:alberto.bemporad@imtlucca.it)

This paper was partially supported by the Italian Ministry of University and Research under the PRIN'17 project "Data-driven learning of constrained control systems", contract no. 2017J89ARP.

of a large number of optimization variables, these approaches are used for offline learning and rely on (batch, mini-batch, or stochastic) gradient descent methods that, although often proved to converge only for convex problems, are widely adopted with success.

To circumvent their very slow convergence and, at the same time, be able to learn NN models incrementally when new data become available, training methods based on extended Kalman filtering (EKF) have been explored in [6] for *feedforward* networks, treating the weight/bias terms of the network as constant states to estimate. When dealing with *recurrent* networks, the authors in [7] distinguish between *parallel*-EKF, which estimates both the hidden states and the weights/bias terms, and *parameter-based* EKF, that only estimates the network parameters, and focus on the latter approach, whose convergence properties were investigated in [8]. Parallel-EKF was also studied in [9] for the special case of having a coincident output and state vector, which is therefore measurable as for NNARX models. In the context of nonlinear filtering, the authors in [10] investigated a parallel-EKF approach for the special case of RNNs that are linear in the input and the output. The method was extended in [11] to make the EKF implementation more efficient by taking into account how much each network parameter affects the predicted output. An ensemble Kalman filter method was proposed in [12]. All the aforementioned EKF-based methods consider quadratic penalties on the output prediction errors and the weight/bias terms of the RNN.

In this paper, we also consider a parallel-EKF approach to recursively learn a general class of RNNs whose state-update and output functions are deep neural networks, under arbitrary convex and twice-differentiable loss functions for penalizing output open-loop prediction errors and for regularizing the weight/bias terms of the RNN, and also extend to the case of  $\ell_1$ -regularization for network topology selection. We also compare EKF to different formulations based on stochastic gradient descent (SGD) methods, in which only the initial state or also the intermediate states of the RNN are treated as optimization variables. We show the superiority of EKF with respect to SGD in a nonlinear identification benchmark and in learning a linear dynamical system with binary outputs. We also explore the use of EKF-based learning for data-driven nonlinear MPC design, showing a relation between the use of constant disturbance models and the adaptation of the bias terms in the neural networks for offset-free tracking, which we illustrate in a nonlinear control benchmark.

## 1.1 Notation

Given a vector  $v \in \mathbb{R}^n$  and a matrix  $A \in \mathbb{R}^{m \times n}$ ,  $v_i$  denotes the  $i$ th real-valued component of  $v$ ,  $A_{i,:}$  the  $i$ th row of  $A$ ,  $A_{:,j}$  its  $j$ th column,  $A_{ij}$  its  $(i, j)$ th entry. Given  $v \in \mathbb{R}^n$  and a symmetric positive semidefinite matrix  $Q = Q' \succeq 0$ ,  $Q \in \mathbb{R}^{n \times n}$ , we denote by  $\|v\|_Q^2$  the quadratic form  $v'Qv$ , by  $\|v\|_1 = \sum_{i=1}^n |v_i|$  the 1-norm of  $v$ , and by  $\text{sign}(v)$  the vector whose  $i$ th component is the sign of  $v_i$ . Given  $a, b \in \mathbb{N}$ ,  $\delta_{a,b}$  denotes the Kronecker delta function ( $\delta_{a,b} = 1$  if  $a = b$  or 0 otherwise).

## 2 Recurrent neural network model

We consider a recurrent neural network (RNN) model with input  $u \in \mathbb{R}^{n_u}$ , predicted output  $\hat{y} \in \mathbb{R}^{n_y}$ , and state vector  $x \in \mathbb{R}^{n_x}$  whose state-update and output equations are feedforward

(deep) neural networks:

$$\left\{ \begin{array}{l} v_1^x(k) = A_1^x \begin{bmatrix} x(k) \\ u(k) \end{bmatrix} + b_1^x \\ v_2^x(k) = A_2^x f_1^x(v_1^x(k)) + b_2^x \\ \vdots \\ v_{L_x}^x(k) = A_{L_x}^x f_{L_x-1}^x(v_{L_x-1}^x(k)) + b_{L_x}^x \\ x(k+1) = v_{L_x}^x(k) \end{array} \right. \quad (1a)$$

$$\left\{ \begin{array}{l} v_1^y(k) = A_1^y \begin{bmatrix} x(k) \\ u(k) \end{bmatrix} + b_1^y \\ v_2^y(k) = A_2^y f_1^y(v_1^y(k)) + b_2^y \\ \vdots \\ v_{L_y}^y(k) = A_{L_y}^y f_{L_y-1}^y(v_{L_y-1}^y(k)) + b_{L_y}^y \\ \hat{y}(k) = f_{L_y}^y(v_{L_y}^y(k)) \end{array} \right. \quad (1b)$$

where  $L_x - 1 \geq 0$  and  $L_y - 1 \geq 0$  are the number of hidden layers of the state-update and output functions, respectively,  $v_i^x \in \mathbb{R}^{n_i^x}$ ,  $i = 1, \dots, L_x - 1$ ,  $v_{L_x}^x \in \mathbb{R}^{n_x}$ , and  $v_i^y \in \mathbb{R}^{n_i^y}$ ,  $i = 1, \dots, L_y$ , the values of the corresponding inner layers,  $f_i^x : \mathbb{R}^{n_i^x} \rightarrow \mathbb{R}^{n_{i+1}^x}$ ,  $i = 1, \dots, L_x - 1$ ,  $f_i^y : \mathbb{R}^{n_i^y} \rightarrow \mathbb{R}^{n_{i+1}^y}$ ,  $i = 1, \dots, L_y - 1$  the corresponding activation functions, and  $f_{L_y}^y : \mathbb{R}^{n_{L_y}^y} \rightarrow \mathbb{R}^{n_y}$  the output function, e.g.,  $f_{L_y}^y(v_{L_y}^y) = v_{L_y}^y$  to model numerical outputs or  $[f_{L_y}^y(v_{L_y}^y)]_i = \left(1 + e^{[v_{L_y}^y]_i}\right)^{-1}$ ,  $i = 1, \dots, n_y$ , for binary outputs. The strict causality of the RNN (1) can be simply imposed by zeroing the last  $n_u$  columns of  $A_1^y$ . The classical *vanilla* (i.e., one-layer) RNN model

$$\begin{aligned} h(k) &= f(W_{1u}v(k) + W_{1h}h(k-1) + b_1) \\ \hat{y}(k) &= W_2h(k) + b_2 \end{aligned} \quad (2)$$

with hidden state vector  $h(k)$  is a special case of (1) obtained by setting  $h(k) = x(k)$ ,  $v(k) = u(k-1)$ ,  $L_x = 2$ ,  $f = f_1^x$ ,  $A_1^x = [W_{1h} \ W_{1u}]$ ,  $b_1 = b_1^x$ ,  $A_2^x = I$ ,  $b_2^x = 0$ ,  $L_y = 1$ ,  $A_1^y = [W_2 \ 0]$ ,  $b_1^y = b_2$ ,  $n_1^y = n_y$ , and  $f_1^y(y) = y$ .

The hyper-parameters describing the RNN (1) are  $n_x$ ,  $\{n_i^x\}$ ,  $\{n_i^y\}$ ,  $\{f_i^x\}$ ,  $\{f_i^y\}$  and dictate the chosen model structure. The parameters to learn are  $A_1^x, \dots, A_{L_x-1}^x, b_1^x, \dots, b_{L_x-1}^x, A_1^y, \dots, A_{L_y-1}^y, b_1^y, \dots, b_{L_y-1}^y$ , where  $A_i^x \in \mathbb{R}^{n_i^x \times n_{i-1}^x}$  is the matrix of weights for layer  $\#i$  of the state-update neural function,  $b_i^x \in \mathbb{R}^{n_i^x}$  the corresponding vector of bias terms, and  $n_0^x \triangleq n_x + n_u$ ,  $n_L^x \triangleq n_x$ , and  $A_i^y \in \mathbb{R}^{n_i^y \times n_{i-1}^y}$  is the matrix of weights for layer  $\#i$  of the output neural function,  $b_i^y \in \mathbb{R}^{n_i^y}$  the corresponding vector of bias terms, and  $n_0^y \triangleq n_x + n_u$ . We denote by  $\theta \in \mathbb{R}^{n_\theta}$  the vector obtained by stacking all the entries of such weight/bias parameters,  $n_\theta \triangleq \sum_{i=1}^{L_x} n_i^x (n_{i-1}^x + 1) + \sum_{i=1}^{L_y} n_i^y (n_{i-1}^y + 1)$ .

We remark that all the results reported in this paper also apply to training *feedforward* neural networks, which is just a special case of (1) for  $n_x = 0$ . Moreover, they can be clearly applied also to identify linear models, that is another special case of (1) when  $L_x = L_y = 1$ ,  $b_1^x = 0$ ,  $b_1^y = 0$ .

### 3 RNN training problem

Consider the following RNN learning problem: Given a training dataset  $\{u(0), y(0), \dots, u(N-1), y(N-1)\}$ , determine an optimal solution  $(x_0^*, \theta^*)$  solving the following mathematical program

$$\begin{aligned} \min_{x_0, \theta} \quad & V(x_0, \theta) \triangleq r_\theta(\theta) + r_x(x_0) + \frac{1}{N} \sum_{k=0}^{N-1} \ell(y(k), \hat{y}(k)) \\ \text{s.t.} \quad & \hat{y}(k) = f_y(\theta, x(k), u(k)) \\ & x(k+1) = f_x(\theta, x(k), u(k)), \quad x(0) = x_0 \end{aligned} \quad (3)$$

where  $f_x(\theta, x(k), u(k))$ ,  $f_y(\theta, x(k), u(k))$  are a condensed form of (1a) and (1b), respectively,  $\ell : \mathbb{R}^{n_y} \times \mathbb{R}^{n_y} \rightarrow \mathbb{R}$  is a loss function penalizing the dissimilarity between the training samples  $y(k)$  and the predicted values  $\hat{y}(k)$  generated by simulating (1), and  $r_\theta : \mathbb{R}^{n_\theta} \rightarrow \mathbb{R}$ ,  $r_x : \mathbb{R}^{n_x} \rightarrow \mathbb{R}$  are regularization functions. In the examples reported in this paper we will consider the (weighted) mean-square error (MSE) loss  $\ell_{\text{MSE}}(y, \hat{y}) = \frac{1}{2} \|y - \hat{y}\|_{W_y}^2$  where  $W_y = W_y' \succ 0$  is weight matrix, the (modified) cross-entropy loss  $\ell_{\text{CE}\epsilon}(y(k), \hat{y}) = \sum_{i=1}^{n_y} -y_i(k) \log(\epsilon + \hat{y}_i) - (1 - y_i(k)) \log(1 + \epsilon - \hat{y}_i)$  for binary outputs, the Tikhonov (or  $\ell_2$ ) regularization terms  $r_\theta(\theta) = \frac{\rho_\theta}{2} \|\theta\|_2^2$ ,  $r_x(x_0) = \frac{\rho_x}{2} \|x_0\|_2^2$  with  $\rho_\theta, \rho_x \geq 0$ , and the  $\ell_1$ -loss  $r_\theta(\theta) = \lambda \|\theta\|_1$ .

#### 3.1 Condensed learning

An optimizer  $(x_0^*, \theta_0^*)$  of Problem (3) can be computed by different unconstrained nonlinear programming (NLP) solvers [13]. For a given value of  $(x_0, \theta)$ , evaluating  $V(x_0, \theta)$  requires processing an *epoch*, i.e., the entire training dataset. Since the cost function in (3) is not separable due to the dynamic constraints (1), a gradient descent method corresponds to the steepest-descent steps

$$\begin{bmatrix} x_0^{t+1} \\ \theta^{t+1} \end{bmatrix} = \begin{bmatrix} x_0^t \\ \theta^t \end{bmatrix} - \alpha_t \begin{bmatrix} \frac{\partial V}{\partial x_0}(x_0^t, \theta^t) \\ \frac{\partial V}{\partial \theta}(x_0^t, \theta^t) \end{bmatrix} \quad (4)$$

where  $\alpha_t$  is the learning rate at epoch  $t = 1, \dots, N_e$ . By applying the chain rule for computing derivatives, the gradient of the objective function with respect to  $(x_0, \theta)$  can be evaluated efficiently by backpropagation through time [14]. However, gradient computation involves well-known issues, for example in the case of the vanilla RNN (2) with  $v, \hat{y}, h \in \mathbb{R}$ , the quantity  $W_{1h} f'$  gets multiplied by itself multiple times, leading to *vanishing gradients* [15] (when  $|W_{1h} f'| < 1$ ) or *exploding gradients* (when  $|W_{1h} f'| > 1$ ), where  $f'$  is the derivative of the activation function  $f$ .

Problem (3) can be interpreted as a finite-horizon optimal control problem with free initial state  $x_0$  (penalized by  $r_x(x_0)$ ), where  $\theta(k) \equiv \theta$  is the vector of manipulated inputs to optimize,  $r_\theta(\theta)$  the corresponding penalty,  $\hat{y}(k)$  the controlled output,  $y(k)$  the output reference,  $u(k)$  a measured disturbance (alternatively,  $x_0$  could be also seen as an input only acting at time  $-1$  to charge  $x(0)$  from  $x(-1) = 0$ ). As well known in solving MPC problems, the effect of *condensing* the problem (a.k.a. “direct single shooting” [16]) by eliminating state variables potentially leads to numerical difficulties. For example in standard linear MPC formulations an unstable linear prediction model  $x(k+1) = Ax(k) + Bu(k)$  leads to a quadratic program with ill-conditioned Hessian matrix, due to the presence of the terms  $A^k$  that appear in constructing the program (cf. [17]).

#### 3.2 Relaxed non-condensed learning

By following the analogy with MPC, problem (3) can be solved in *non-condensed* form (a.k.a. “direct multiple shooting” [18]) by also treating  $x(1), \dots, x(N-1)$  (and possibly also  $v_i^x(k)$ ,

$v_j^y(k)$ ) as additional optimization variables, subject to the equality constraints imposed by the RNN model equations (1). By further relaxing the model equations we get the following unconstrained nonlinear optimization problem

$$\begin{aligned} \min_{x_0, \theta} \quad & r_\theta(\theta) + r_x(x_0) + \frac{1}{N} \sum_{k=0}^{N-1} \ell(y(k), f_y(\theta, x_k, u(k))) \\ & x_1, \dots, x_{N-1} \\ & + \frac{\gamma}{2N} \sum_{k=0}^{N-2} \|x_{k+1} - f_x(\theta, x_k, u(k))\|_2^2 \end{aligned} \quad (5)$$

where  $\gamma > 0$  is a scalar penalty promoting the consistency of the state sequence with the RNN model equations (1a).

Note that in the case of MSE loss and  $\ell_2$ -regularization, (5) can be solved as a nonlinear least-squares problem, for which efficient solution methods exist [13]. The relaxation (5) is also amenable for stochastic gradient-descent iterations that only update  $(x_k, x_{k+1}, \theta)$  when sample  $k$  is processed:

$$\begin{aligned} \begin{bmatrix} x_{k+1}^{k+1} \\ x_k^{k+1} \\ \theta^{k+1} \end{bmatrix} &= \begin{bmatrix} x_{k+1}^k \\ x_k^k \\ \theta^k \end{bmatrix} - \alpha_k \begin{bmatrix} 0 \\ \frac{\partial \ell}{\partial x}(y(k), f_y(\theta^k, x_k^k, u(k))) \\ \frac{\partial \ell}{\partial \theta}(y(k), f_y(\theta^k, x_k^k, u(k))) \end{bmatrix} \\ &- \gamma \alpha_k \begin{bmatrix} I \\ \frac{\partial f_x}{\partial x}(\theta, x_k^k, u(k))' \\ \frac{\partial f_x}{\partial \theta}(\theta, x_k^k, u(k))' \end{bmatrix} (x_{k+1} - f_k) - \frac{\alpha_k}{N} \begin{bmatrix} 0 \\ \nabla r_x(x_0^k) \delta_{k,0} \\ \nabla r_\theta(\theta^k) \end{bmatrix} \end{aligned} \quad (6)$$

where  $f_k \triangleq f_x(\theta^k, x_k^k, u(k))$ ,  $k = 0, \dots, N-1$ . Clearly, (6) can be also run on multiple epochs by resetting  $k = 0$  at each epoch  $t = 1, \dots, N_e$ .

### 3.3 Relaxed partially-condensed learning

The non-condensed form (5) has  $n_\theta + Nn_x$  optimization variables, where in the present context of control-oriented RNN models usually  $Nn_x \gg n_\theta$ . *Partial condensing* [19] can reduce the training problem as follows. Let us split the dataset into  $M$  batches,  $M \leq N$ , of lengths  $L_1, \dots, L_M$ , respectively (for example,  $L_1 = L_2 = \dots = L_{M-1} = \lceil \frac{N}{M} \rceil$ ,  $L_M = N - (M-1)\lceil \frac{N}{M} \rceil$ ). Then, we solve the following problem:

$$\begin{aligned} \min_{x_0, x_1, \dots, x_{M-1}, \theta} \quad & \frac{1}{N} \sum_{j=0}^{M-1} \sum_{h=0}^{L_j-1} \ell(y(k_{ij}), f_y(\theta, \hat{x}_{h|j}, u(k_{ij}))) \\ & + r_\theta(\theta) + r_x(x_0) + \gamma \frac{N-1}{2N(M-1)} \sum_{j=0}^{M-2} \|x_{j+1} - \hat{x}_{L_j|j}\|_2^2 \end{aligned} \quad (7)$$

where  $k_{ij} \triangleq h + \sum_{s=0}^{j-1} L_s$  and  $\hat{x}_{h|j}$  is the hidden state predicted by iterating (1a) over  $h$  steps from the initial condition  $x_j$  under the input excitation  $u(L_j), \dots, u(L_j + h - 1)$ ,  $h = 1, \dots, L_j$ ,  $j = 0, \dots, M-1$ . Similarly to the approach of [5], problem (7) can be solved by a SGD method by processing  $L_j$  samples at the time, that results in updating  $x_{j+1}, x_j, \theta$  at each SGD iteration. Note that (7) includes (5) as a special case by setting  $M = N$ ,  $L_j \equiv 1$ , and (3) for  $M = 1$ ,  $L_1 = N$ .

## 4 Training by Extended Kalman filtering

To address both the *recursive* estimation of  $\theta$  from real-time streams of input and output measurements and counteract the slow convergence of SGD methods, we consider the use of extended Kalman filtering (EKF) techniques as in [10, 11] to recursively update  $\theta$  and the current hidden state vector. To this end, let us rewrite model (1) as the following nonlinear system affected by noise

$$\begin{aligned} x(k+1) &= f_x(\theta(k), x(k), u(k)) + \xi(k) \\ y(k) &= f_y(\theta(k), x(k), u(k)) + \zeta(k) \\ \theta(k+1) &= \theta(k) + \eta(k) \end{aligned} \quad (8)$$

where  $\xi(k) \in \mathbb{R}^{n_x}$ ,  $\zeta(k) \in \mathbb{R}^{n_y}$ , and  $\eta(k) \in \mathbb{R}^{n_\theta}$  are white, zero-mean, noise vectors with covariance matrices  $Q_x(k)$ ,  $Q_y(k)$ , and  $Q_\theta(k)$ , respectively, with  $Q_x(k) = Q_x(k)' \succeq 0$ ,  $Q_x(k) \in \mathbb{R}^{n_x \times n_x}$ ,  $Q_y(k) = Q_y(k)' \succ 0$ ,  $Q_y(k) \in \mathbb{R}^{n_y \times n_y}$ ,  $Q_\theta(k) = Q_\theta(k)' \succ 0$ ,  $Q_\theta(k) \in \mathbb{R}^{n_\theta \times n_\theta}$  for all  $k$ .

The model coefficients  $\hat{\theta}(k)$  and the hidden state  $\hat{x}(k)$  are estimated with data up to time  $k$  according to the following classical EKF recursive updates:

$$\begin{aligned} C(k) &= \left[ \begin{array}{cc} \frac{\partial f_y}{\partial x} & \frac{\partial f_y}{\partial \theta} \end{array} \right] \Big|_{\hat{\theta}(k|k-1), \hat{x}(k|k-1), u(k)} \\ M(k) &= P(k|k-1)C(k)'[C(k)P(k|k-1)C(k)' + Q_y(k)]^{-1} \\ e(k) &= y(k) - f_y(\hat{\theta}(k|k-1), \hat{x}(k|k-1), u(k)) \\ \begin{bmatrix} \hat{x}(k|k) \\ \hat{\theta}(k|k) \end{bmatrix} &= \begin{bmatrix} \hat{x}(k|k-1) \\ \hat{\theta}(k|k-1) \end{bmatrix} + M(k)e(k) \\ P(k|k) &= (I - M(k)C(k))P(k|k-1) \\ \hat{x}(k+1|k) &= f_x(\hat{\theta}(k|k), \hat{x}(k|k), u(k)) \\ A(k) &= \left[ \begin{array}{cc} \frac{\partial f_x}{\partial x} & \frac{\partial f_x}{\partial \theta} \\ 0 & I \end{array} \right] \Big|_{\hat{\theta}(k|k), \hat{x}(k|k), u(k)} \\ P(k+1|k) &= A(k)P(k|k)A(k)' + \begin{bmatrix} Q_x(k) & 0 \\ 0 & Q_\theta(k) \end{bmatrix} \end{aligned} \quad (9)$$

Let us recall the equivalence between the EKF (9) and Newton's method [20, Sect. 5.2] for solving (5) in the case of loss  $\ell_{\text{MSE}}$  and  $\ell_2$ -regularization, and of an additional penalty on updating  $\theta$ :

$$\begin{aligned} \min_{\substack{x_0, x_1, \dots, x_{N-1} \\ \theta_0, \theta_1, \dots, \theta_{N-1}}} & \frac{1}{2} \left\| \begin{bmatrix} x_0 \\ \theta \end{bmatrix} - \begin{bmatrix} x(0|-1) \\ \theta(0|-1) \end{bmatrix} \right\|_{P(0|-1)^{-1}}^2 \\ & + \frac{1}{2} \sum_{k=0}^{N-1} \|y(k) - f_y(\theta, x_k, u(k))\|_{Q_y^{-1}(k)}^2 \\ & + \frac{1}{2} \sum_{k=1}^{N-2} \|x_{k+1} - f_x(\theta, x_k, u(k))\|_{Q_x^{-1}(k)}^2 \\ & + \|\theta_{k+1} - \theta_k\|_{Q_\theta^{-1}(k)}^2 \end{aligned} \quad (10)$$

By dividing the cost function in (10) by  $N$ , we have that  $Q_x = \frac{1}{\gamma}I$ ,  $Q_y = W_y^{-1}$ , while  $Q_\theta(k) = \frac{1}{\alpha_k}I$  defines a learning-rate due to minimizing the additional term  $\frac{\alpha_k}{2} \|\theta_{k+1} - \theta_k\|_2^2$ . The initial vector  $\begin{bmatrix} x(0) \\ \theta(0) \end{bmatrix}$ , which is treated as a random vector with mean  $\begin{bmatrix} x(0|-1) \\ \theta(0|-1) \end{bmatrix}$  and covariance  $P(0|-1) = P(0|-1)' \succeq 0$ ,  $P(0|-1) \in \mathbb{R}^{(n_x+n_\theta) \times (n_x+n_\theta)}$ . By the analogy between EKF and Newton's

method, we have that

$$P(0| - 1) = \begin{bmatrix} \frac{1}{N\rho_x}I & 0 \\ 0 & \frac{1}{N\rho_\theta}I \end{bmatrix} \quad (11)$$

is directly related to the  $\ell_2$ -regularization terms  $r_\theta(\theta) = \frac{\rho_\theta}{2}\|\theta\|_2^2$ ,  $r_x(x_0) = \frac{\rho_x}{2}\|x_0\|_2^2$  used in (5) when  $x(0| - 1) = 0$ ,  $\theta(0| - 1) = 0$ .

In the next section, we show how to extend EKF-based training to handle generic strongly convex and twice differentiable loss functions  $\ell$  and regularization terms  $r_\theta, r_x$ .

#### 4.1 EKF with general output prediction loss

**Lemma 1** *Let  $\ell : \mathbb{R}^{n_y} \times \mathbb{R}^{n_y} \rightarrow \mathbb{R}$  be strongly convex and twice differentiable with respect to its second argument  $\hat{y}$ . Then by setting*

$$Q_y(k) \triangleq \frac{\partial^2 \ell(y(k), \hat{y}(k|k-1))^{-1}}{\partial \hat{y}^2} \quad (12a)$$

$$e(k) = -Q_y(k) \frac{\partial \ell(y(k), \hat{y}(k|k-1))}{\partial \hat{y}} \quad (12b)$$

the EKF updates (9) attempt at minimizing the loss  $\ell$ .

*Proof.* At each step  $k$ , let us take a second-order Taylor expansion of  $\ell(y(k), \hat{y})$  around  $\hat{y}(k|k-1)$  to approximate

$$\begin{aligned} \arg \min \ell(y(k), \hat{y}) &\approx \arg \min \left\{ \frac{1}{2} \Delta y'_k Q_y^{-1}(k) \Delta y_k \right. \\ &\quad \left. + \varphi'_k \Delta y_k \right\} \\ &= \arg \min \left\{ \frac{1}{2} \|\hat{y}(k|k-1) - Q_y(k) \varphi_k - \hat{y}\|_{Q_y^{-1}(k)}^2 \right\} \end{aligned} \quad (13)$$

where  $\Delta y_k = \hat{y} - \hat{y}(k|k-1)$  and  $\varphi_k \triangleq \frac{\partial \ell(y(k), \hat{y}(k|k-1))}{\partial \hat{y}}$ .

Due to the parallel between EKF and Newton's method recalled in (10), feeding the measured output  $y(k) = \hat{y}(k|k-1) - Q_y(k) \varphi_k$  gives  $e(k)$  and  $Q_y(k)$  as in (12).  $\square$

**Remark 1** *Note that for the MSE loss  $\ell_{\text{MSE}}(y(k), \hat{y}) = \frac{1}{2} \|y(k) - \hat{y}\|_{W_y}^2$ , as  $Q_y(k) = W_y^{-1}$ , we get  $\varphi_k = Q_y^{-1}(k)(\hat{y}(k|k-1) - y(k))$  and hence from (12b) the classical output prediction error term  $e(k) = y(k) - \hat{y}(k|k-1)$ .  $\square$*

**Remark 2** *When the modified cross-entropy loss  $\ell_{\text{CE}\epsilon}(y(k), \hat{y})$  is used to handle binary outputs  $y(k) \in \{0, 1\}$  and predictors  $\hat{y}(k|k-1) \in [0, 1]$  we get  $\varphi_k = -\frac{y(k)}{\epsilon + \hat{y}(k|k-1)} + \frac{1-y(k)}{1+\epsilon - \hat{y}(k|k-1)}$  and*

$$Q_y(k) = \left( \frac{y(k)}{(\epsilon + \hat{y}(k|k-1))^2} + \frac{1-y(k)}{(1+\epsilon - \hat{y}(k|k-1))^2} \right)^{-1} \quad (14a)$$

Hence, from (12b), we get  $e(k) = -1 - \epsilon - \hat{y}(k|k-1)$  for  $y(k) = 0$  and  $e(k) = \epsilon + \hat{y}(k|k-1)$  for  $y(k) = 1$ , or equivalently

$$e(k) = (1 + 2\epsilon)y(k) + \hat{y}(k|k-1) - 1 - \epsilon \quad (14b)$$

Note that  $\epsilon > 0$  is used to avoid possible numerical issues in computing  $Q_y^{-1}(k)$  when  $\hat{y}(k|k-1)$  tends to 0 or 1.  $\square$

## 4.2 EKF with generic regularization terms

We have seen in (11) how a quadratic regularization  $r_\theta$  can be embedded in the EKF formulation by properly defining  $P(0|-1)$ . We now extend the formulation to handle more general regularization terms.

**Lemma 2** *Consider the generic regularization term*

$$r_\theta(\theta) = N\Psi(\theta) + \frac{1}{2}\rho_\theta\|\theta\|_2^2$$

and let  $\Psi : \mathbb{R}^{n_\theta} \rightarrow \mathbb{R}$  be strongly convex and twice differentiable. Then by extending model (8) with the additional system output

$$y_\Psi(k) = \theta(k) + \mu_\Psi(k) \quad (15)$$

where  $\mu_\Psi(k)$  has zero mean and covariance

$$Q_\Psi(k) = \nabla_\theta^2 \Psi(\theta(k|k-1))^{-1} \quad (16a)$$

and by feeding the error term

$$e_\Psi(k) = -Q_\Psi(k)\nabla_\theta \Psi(\theta(k|k-1)) \quad (16b)$$

the EKF updates (9) attempt at minimizing  $r_\theta(x_0)$ .

*Proof.* At a given prediction step  $k$ , consider the approximate minimization of  $\Psi$  around  $\theta(k|k-1)$

$$\begin{aligned} \arg \min \Psi(\theta) &\approx \arg \min \left\{ \frac{1}{2} \Delta\theta'_k Q_\Psi^{-1} \Delta\theta_k + \gamma'_k \Delta\theta_k \right\} \\ &= \arg \min \left\{ \frac{1}{2} \|\Delta\theta_k + Q_\Psi(k)\gamma_k\|_{Q_\Psi^{-1}(k)}^2 \right\} \end{aligned}$$

where  $\Delta\theta_k \triangleq \theta - \theta(k|k-1)$  and  $\gamma_k \triangleq \nabla_\theta \Psi(\theta(k|k-1))$ . By feeding the measurement  $y_\Psi(k) = \theta(k|k-1) - Q_\Psi^{-1}(k)\gamma_k$  to the EKF, as in (12) we get the additional error term  $e_\Psi(k) = -Q_\Psi(k)\gamma_k$  and the corresponding output Jacobian matrix  $C_\Psi(k) = [0 \ I]$ .  $\square$

Note that for  $\Psi(\theta) = \frac{1}{2}\bar{\rho}_\theta \sum_{i=1}^{n_\theta} \theta_i^2$ , then  $Q_\Psi(k) = \frac{1}{\bar{\rho}}I$  and  $e_\Psi(k) = -\hat{\theta}(k|k-1)$ . Next Lemma 3 specializes the result of Lemma 2 to a wider class of separable regularization functions.

**Lemma 3** *Let  $\Psi(\theta) = \sum_{i=1}^{n_\theta} \psi_i(\theta_i)$  and assume that each function  $\psi_i : \mathbb{R} \rightarrow \mathbb{R}$  is strongly convex and twice differentiable. Then minimizing the additional loss  $\Psi$  corresponds to adding the following further updates in the EKF (9)*

$$\begin{aligned} C_{\Psi_i}(k+h_i) &= I_{i,:} \\ e_{\Psi_i}(k+h_i) &= -\frac{\psi'_i(\hat{\theta}_i(k|k+h_{i-1}))}{\psi''_i(\hat{\theta}_i(k|k+h_{i-1}))} \\ M(k+h_i) &= \frac{P_{:,i}(k+h_i|k+h_{i-1})}{P_{ii}(k+h_i|k+h_{i-1}) + \psi''_i(\hat{\theta}_i(k+h_{i-1}|k+h_{i-1}))^{-1}} \\ \begin{bmatrix} \hat{x}(k+h_i|k+h_i) \\ \hat{\theta}(k+h_i|k+h_i) \end{bmatrix} &= \begin{bmatrix} \hat{x}(k+h_i|k+h_{i-1}) \\ \hat{\theta}(k+h_i|k+h_{i-1}) \end{bmatrix} \\ &\quad + M(k+h_i)e_{\Psi_i}(k+h_i) \\ P(k+h_i|k+h_i) &= P(k+h_i|k+h_{i-1}) \\ &\quad - M(k+h_i)P_{n_x+i,:}(k+h_i|k+h_{i-1}) \end{aligned} \quad (17)$$

after each measurement update  $k$ , where  $h_i = -1 + \frac{n_y+i}{n_y+n_\theta}$ ,  $i = 0, \dots, n_\theta$ .



*Proof.* The result simply follows due to the independence of each component  $\mu_{\Psi_i}(k)$  in (15),  $i = 1, \dots, n_\theta$ , and  $\zeta(k)$  in (8), see, e.g., [21, Sect. 10.2.1]. In fact, the multi-output measurement update of the EKF can be processed sequentially, i.e., first  $y(k)$  and then one output  $y_{\Psi_i}(k)$  at the time. Denote by  $\hat{\theta}(k|i+k-h_i)$  the estimate of  $\theta(k)$  after the first  $i$  measurements  $y_{\Psi_i}(k)$  have been processed. Then, when processing the  $i$ th component of  $y_\Psi$ , we get the updates in (17).  $\square$

### 4.3 EKF-based training with $\ell_1$ -regularization

When training RNN models several degrees of freedom exist in selecting the model structure, i.e., the number of layers and of neurons in each layer of the feedforward neural networks  $f_x, f_y$ . It is common to start with a large enough number of parameters and then promote the sparsity of  $\theta$  by introducing an  $\ell_1$ -penalty  $r_\theta(\theta) = \lambda N \|\theta\|_1$ . We next show how to handle such a sparsifier in our EKF-based setting.

**Lemma 4** *Minimizing the additional loss  $\lambda N \|\theta\|_1$  on  $\theta$  corresponds to modifying the measurement update for  $\hat{x}(k|k)$  and  $\hat{\theta}(k|k)$  in (9) into*

$$\begin{bmatrix} \hat{x}(k|k) \\ \hat{\theta}(k|k) \end{bmatrix} = \begin{bmatrix} \hat{x}(k|k-1) \\ \hat{\theta}(k|k-1) \end{bmatrix} + M(k)C(k) - \lambda P(k|k-1) \begin{bmatrix} 0 \\ \text{sign}(\hat{\theta}(k|k-1)) \end{bmatrix} \quad (18)$$

*Proof.* Let us consider the following smooth version of the 1-norm  $\Psi(\theta) = \lambda \sum_{i=1}^{n_\theta} \sqrt{\theta_i^2 + \tau}$  and the associated derivatives  $\psi'_i(\theta_i) = \lambda \theta_i (\tau + \theta_i^2)^{-\frac{1}{2}}$ ,  $\psi''_i(\theta_i) = \lambda \tau (\tau + \theta_i^2)^{-\frac{3}{2}}$ . By applying Lemma 3 we get the following updates  $e_{\Psi_i}(k+h_i) = -\frac{\hat{\theta}_i}{\tau} \left( \tau + \hat{\theta}_i^2 \right)$ ,  $M(k+h_i) = \frac{\lambda \tau P_{:,i}}{\lambda \tau P_{:,i} + (\tau + \hat{\theta}_i^2)^{\frac{3}{2}}}$  where we omitted “ $(k+h_i|k+h_{i-1})$ ” for simplicity of reading. For  $\tau \rightarrow 0$  we get  $M(k+h_i)e_{\Psi_i}(k+h_i) \rightarrow \frac{\lambda \hat{\theta}_i^3 P_{:,i}}{(\hat{\theta}_i^2)^{\frac{3}{2}}} = \lambda \text{sign}(\hat{\theta}_i(k|k+h_{i-1}))P_{:,i}$ . Moreover,  $M(k+h_i) \rightarrow 0$  and hence the measurement update of  $P(k+h_i|k+h_i)$  in (17) is ineffective, i.e.,  $P(k+h_i|k+h_i) - P(k+h_i|k+h_{i-1}) \rightarrow 0$ . The result in (18) then follows by applying the recursions in (17) for  $i = 1, \dots, n_\theta$ .  $\square$

### 4.4 Initial state reconstruction

Given a model  $\theta$  and a dataset  $\{\bar{u}(0), \bar{y}(0), \dots, \bar{u}(\bar{N}-1), \bar{y}(\bar{N}-1)\}$ , testing the prediction capabilities of the model in open-loop simulation requires determining an appropriate initial state  $\bar{x}(0)$ . A way to get  $\bar{x}(0)$  is to solve the following state-reconstruction problem with  $n_x$  variables

$$\min_{\bar{x}_0} r_x(x_0) + \frac{1}{\bar{N}} \sum_{k=0}^{\bar{N}-1} \ell(\bar{y}(k), \hat{y}(k)) \quad (19)$$

where  $\hat{y}(k)$  are generated by iterating (1) with from  $x(0) = \bar{x}_0$ , or its equivalent non-condensed or partially-condensed form.

Solving (19) is not only useful to test a trained model on new data, but also when running the EKF (9) offline on training data over multiple epochs. In this case, Problem (19) can provide a suitable value for  $x(0|-1)$  for the new epoch based on the last vector  $\hat{\theta}(N-1|N-1)$  learned, that is used in (19) and as the initial condition  $\theta(0|-1)$  for the new epoch. We remark that when the EKF is run on  $N_e$  epochs and  $P(0|-1)$  is set equal to the value  $P(N|N-1)$  from the previous epoch, in (11) one should divide by  $N_e N$  and not by  $N$  for consistency.

## 5 Nonlinear model predictive control

In a fully adaptive case, the EKF as in (9) can be used online both to estimate the state and to update the parameters of the model from streaming output measurements. Then, a nonlinear MPC controller can be setup by solving a finite-time nonlinear optimal control problem over the horizon  $[k, k+p]$  at each execution time  $k$  for a given prediction horizon  $p$ , taking  $\hat{x}(k|k)$  as the initial state of the prediction and using  $\hat{\theta}(k|k)$  to make nonlinear predictions. An example of such an adaptive nonlinear MPC scheme, that we will use in the numerical experiments reported in Section 6, is

$$\begin{aligned} \min_{u_0, \dots, u_{p-1}} \quad & \sum_{t=0}^p \|W^{\Delta u}(u_t - u_{t-1})\|_2^2 + \|W^y(y_t - r_t)\|_2^2 \\ \text{s.t.} \quad & x_{t+1} = f_x(\hat{\theta}(k|k), x_t, u_t), \quad y_t = f_y(\hat{\theta}(k|k), x_t, u_t) \\ & u_{\min} \leq u_t \leq u_{\max} \end{aligned} \quad (20)$$

where  $x_0 = x(k|k)$  and  $u_{-1} = u(k-1)$ . Note that the last penalty on  $u_p - u_{p-1}$  and the first penalty on  $y_0 - r_0$  in (20) can be omitted in case of strictly-causal RNN models.

When full adaptation is not recommended, for instance to prevent excessive changes of the model parameters and/or to avoid computing the full EKF iterations, a non-adaptive nonlinear MPC setting can be used, in which an optimal vector  $\theta^*$  of parameters is obtained offline by running (9) on a training input/output dataset and used to make model-based predictions. A possible drawback of the latter approach is that offsets may arise in steady state when tracking constant set-points due to model/plant mismatches. A common practice is to augment the observer with a disturbance model [22, 23], that in the current nonlinear MPC setting corresponds to augment the prediction model as follows (cf. [24]):

$$\begin{aligned} x(k+1) &= f_x(\theta(k), x(k), u(k)) + B_d d(k) + \xi(k) \\ y(k) &= f_y(\theta(k), x(k), u(k)) + C_d d(k) + \zeta(k) \\ d(k+1) &= d(k) + \eta(k) \end{aligned} \quad (21)$$

and estimate  $\hat{x}(k|k)$ ,  $d(k|k)$  by EKF. Clearly, such a solution corresponds to only updating the bias terms  $b_1^x$ ,  $b_{L_y}^y$  of the RNN model (1) by setting  $b_1^x(k|k) = (b_1^x)^* + B_d d(k|k)$ ,  $b_{L_y}^y(k|k) = (b_{L_y}^y)^* + C_d d(k|k)$ . The (frequently used) case of pure output disturbance models ( $B_d = 0$ ,  $C_d = I$ ) corresponds to only updating  $b_{L_y}^y$ .

## 6 Numerical experiments

We test the proposed RNN learning algorithms on system identification and nonlinear MPC problems. All computations have been carried out in Python 3.8.10 on an Intel Core i9-10885H CPU @2.40GHz machine using PyTorch [25], with no particular care of code efficiency and numerical robustness of the EKF iterations (cf. [21]). In all numerical tests, unless stated differently, we use covariance matrices  $Q_x(k) \equiv 0$ ,  $Q_\theta(k) \equiv 0$ ,  $Q_y(k) \equiv 1$ ,  $P(0|-1) = I$  (i.e.,  $\rho_x = \rho_\theta = \frac{1}{N_e N}$ , where  $N_e$  is the number of epochs the EKF is run), and initial state  $x(0|-1) = 0$ , unless stated differently. Standard scaling of the input and output samples is performed by computing their means and standard deviations on training data. Model quality is judged in terms of the original data by the normalized root-mean-square error (NRMSE) =  $100 \frac{1 - \frac{\|Y - \hat{Y}\|_2}{\|Y - \bar{y}\|_2}}{\|Y - \bar{y}\|_2}$  for numeric outputs, where  $Y$  is the vector of measured output samples,  $\hat{Y}$  the vector of output samples simulated by the identified model fed in open-loop with the input data, and  $\bar{y}$  is the mean of  $Y$ , and by the accuracy

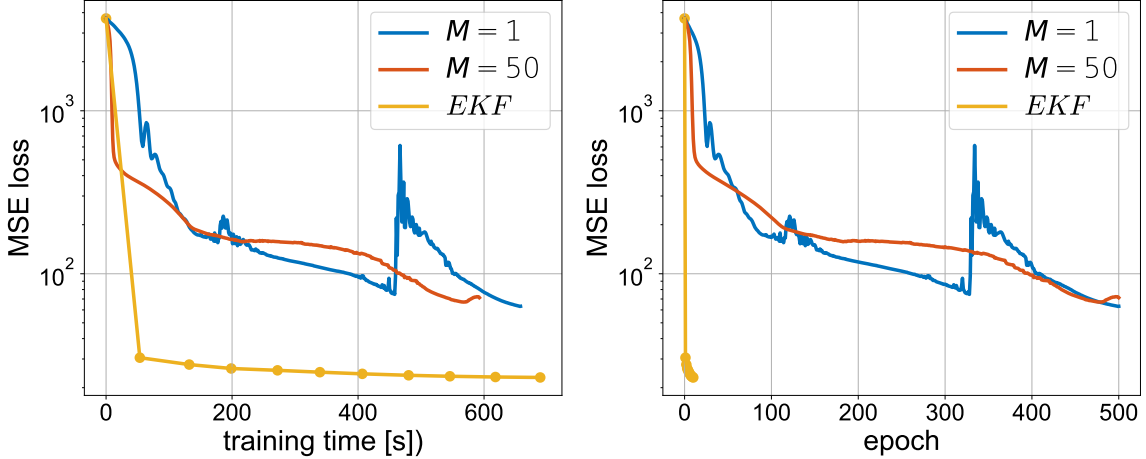


Figure 1: Fluid damper benchmark: training loss  $V(x_0, \theta)$  evaluated at each epoch

$a = \frac{1}{N} \sum_{k=1}^N \delta_{\hat{y}_b(k), y(k)}$  for binary outputs, where  $\hat{y}_b(k) = 0$  if  $\hat{y}(k) < 0.5$  or 1 otherwise. In all tests, Problem (19) is solved with  $\bar{N} = 100$  by PyTorch’s implementation of AMSgrad [26] with learning rate  $l_r = 0.1$  over 100 epochs. In all tests, when running the EKF, most of the CPU time is spent in computing the Jacobian matrices w.r.t.  $(x, \theta)$ , that largely dominates over the cost for the linear algebra operations in (9).

## 6.1 Fluid damper benchmark

We consider the nonlinear black-box modeling of the dynamic behavior of a magneto-rheological fluid damper [27]. As in the demo problem of nonlinear autoregressive (NARX) model identification in the System Identification (SYS-ID) Toolbox for MATLAB R2021a [28], we use  $N = 2000$  data for training, the remaining 1499 for testing. We consider a RNN model with  $n_x = 4$  hidden states and shallow state-update and output network functions ( $L_x = L_y = 2$ ) with  $n_1^x = n_1^y = 6$  neurons, leaky-ReLU activation functions  $f_1^x, f_1^y$  with negative slope = 0.01, and linear output function  $f_2^y$ . The EKF-based learning method is run on multiple epochs and compare the results to those obtained by using AMSgrad with learning rate  $l_r = 0.01$  to solve the fully condensed problem (3), and  $l_r = 0.0005$  for the partially-condensed problem (7) with  $M = 50$ .

Figure 1 shows the value of the MSE loss  $V(x_0, \theta)$  obtained by running the algorithms on multiple epochs. When using EKF, in order to compute  $V(x_0, \theta)$  after each epoch the initial condition  $x_0$  is reconstructed by solving (19) with  $\bar{u}(k) = u(k)$ ,  $\bar{y}(k) = y(k)$ . It is apparent that EKF reaches a good-quality model already after one pass through the training dataset and outperforms the other methods. Another advantage of EKF is that little effort was put on tuning the covariance matrices  $Q_y, Q_x, Q_\theta, P(0| - 1)$  for the EKF, while AMSgrad required a careful tuning of the learning rate  $l_r$  and also of the penalty  $\gamma$  in case  $M > 1$ . The first 10 components of the estimated parameter vector  $\hat{\theta}(k|k) \in \mathbb{R}^{101}$  are plotted in Figure 2. Figure 3 shows open-loop simulations on test data by the EKF-trained model and by the best model `Narx_6_2` reported in [28]. The NRMSE obtained by `Narx_6_2` is 88.18% on training data and 85.15% on test data, while RNN achieves 91.81% on training data and 90.84% on test data. For  $M = 1$  ( $M = 50$ ), the NRMSE achieved by AMSgrad, when collecting the model that gives the minimum  $V(x_0, \theta)$  during gradient descent, is 86.46% (86.04%) on training data and 82.30% (82.40%) on test data.

In Figure 4 we show the NRMSE obtained when  $\ell_1$ -regularization is introduced in the EKF as in (18) for different values of  $\lambda$ . The same figure also shows the percentage of zero entries in the

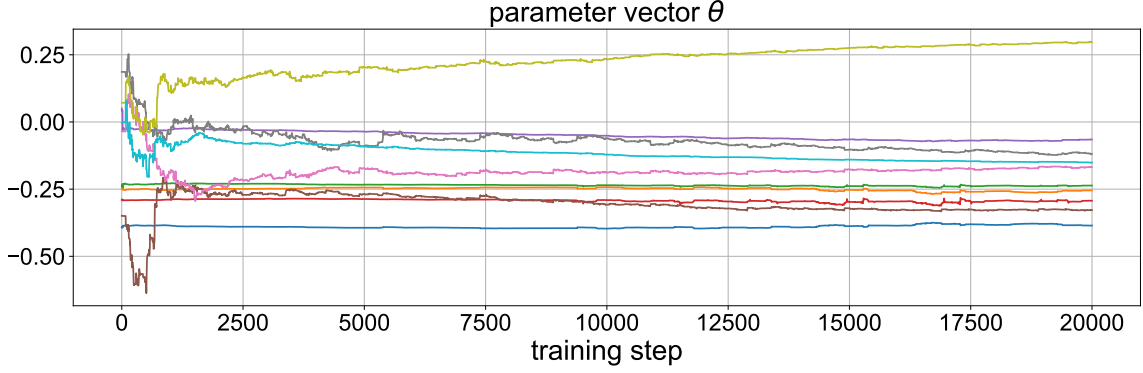


Figure 2: Fluid damper benchmark:  $\hat{\theta}_i(k|k)$  (first 10 parameters only) over 10 epochs of 2000 samples each

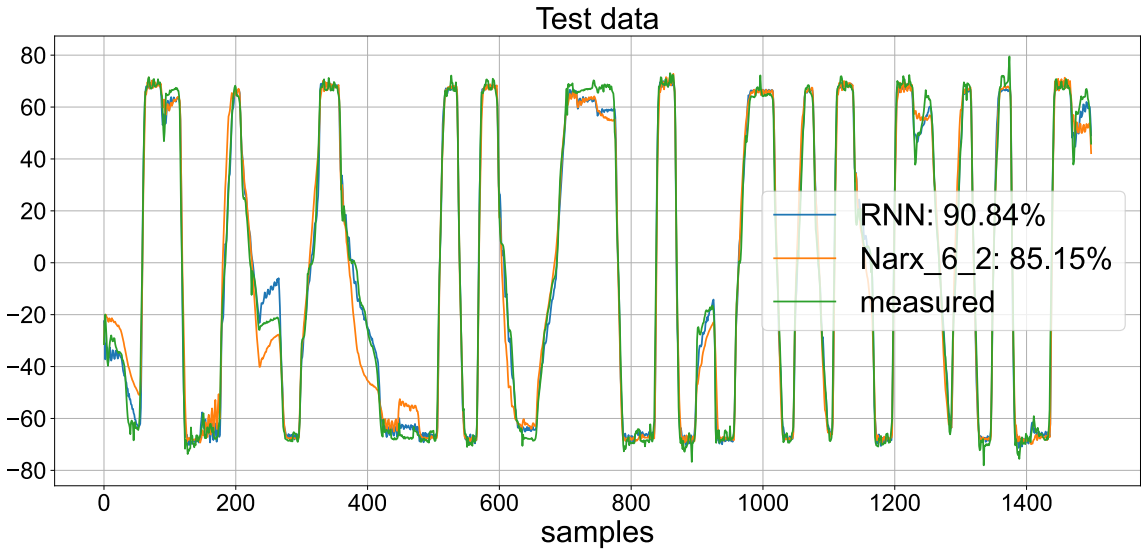


Figure 3: Fluid damper benchmark: NRMSE on test data

resulting parameter vector  $\theta$ , where each entry  $\theta_i$  such that  $|\theta_i| \leq 10^{-3}$  is set to zero after EKF training. As expected, for increasing values of  $\lambda$  the parameter vector gets more sparse, at the price of decreased prediction quality. For large values of  $\lambda$  (roughly  $\lambda > 2$ ), results start deteriorating, possibly due to the excessively large steps taken in (18) that mine the convergence of the EKF.

## 6.2 Linear dynamical system with binary outputs

Consider 2000 input/output pairs generated by the following linear system with binary outputs

$$\begin{aligned}
 x(k+1) &= \begin{bmatrix} .8 & .2 & -.1 \\ 0 & .9 & .1 \\ .1 & -.1 & .7 \end{bmatrix} x(k) + \begin{bmatrix} -.1 \\ .5 \\ 1 \end{bmatrix} u(k) + \xi(k) \\
 y(k) &= \begin{cases} 1 & \text{if } [-2.0 \ 1.5 \ 0.5] x(k) + \zeta(k) \geq 0 \\ 0 & \text{otherwise} \end{cases}
 \end{aligned}$$

from  $x(0) = 0$ , with the values of the input  $u(k)$  changed with 90% probability from step  $k$  to  $k+1$  with a new value drawn from the uniform distribution on  $[0, 1]$ . The disturbances  $\xi_i(k), \zeta(k) \sim \mathcal{N}(0, \sigma^2)$ ,  $i = 1, 2, 3$ , are assumed independent. We consider the first  $N = 1000$  samples for

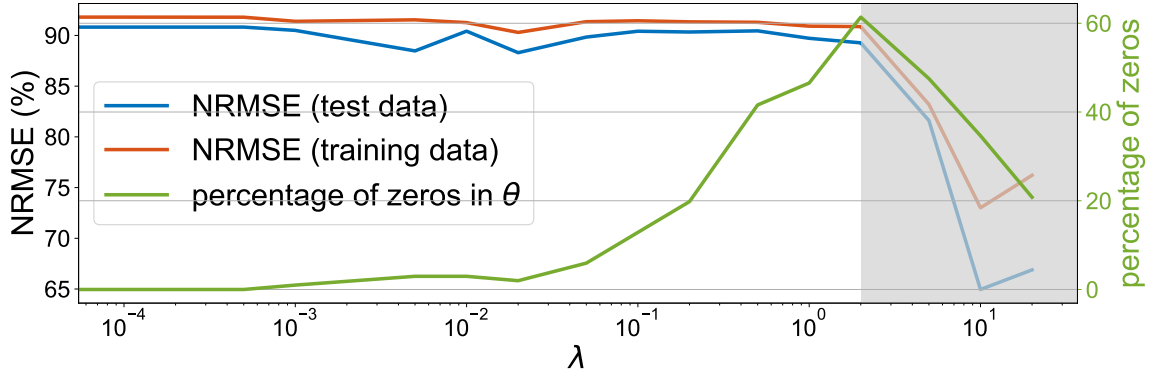


Figure 4: Fluid damper benchmark: NRMSE and sparsity of  $\theta$  optimized by EKF vs  $\ell_1$ -regularization coefficient  $\lambda$

training, the rest for testing. We want to fit an affine model ( $L_x = L_y = 1$ ) with sigmoidal output function  $f_1^y(y) = 1/(1 + e^{A_1^y[x'(k) u(k)]' + b_1^y})$ . Output data are not scaled.

We run EKF over 10 epochs and AMSGrad over 500 epochs with the same settings as in Section 6.1, modified cross-entropy loss  $\ell_{CE\epsilon}$  for  $\epsilon = 10^{-2}$ , and EKF updates as in (14). For best accuracy results, AMSGrad-based training is run with  $\rho_x = \rho_\theta = 10^{-4}$  and learning rates selected by trial and error as  $l_r = 0.02$  ( $l_r = 0.002$ ) for  $M = 1$  ( $M = 50$ ) to trade off convergence rate and variance. The results obtained for  $\sigma = 0$  are shown in Figure 5, where it is again apparent the superior convergence quality of EKF with respect to gradient descent. To test the robustness of the methods against noisy data, we repeat the experiment for increasing values of  $\sigma$ . Table 1 shows the accuracy obtained by EKF and AMSGrad (for  $M = 1$  and  $M = 50$ ). Note that we kept  $Q_x = 0$  in all tests, as we assumed not to know the intensity of the disturbances entering the system.

$\sigma$	$M = 1$	$M = 50$	EKF
0.000	93.90 (99.40)	94.50 (98.70)	99.40 (100.00)
0.001	93.90 (99.40)	94.50 (98.70)	99.40 (100.00)
0.010	93.80 (99.50)	94.60 (98.20)	99.10 (99.90)
0.100	93.10 (97.30)	93.30 (81.70)	95.40 (97.80)
0.200	91.80 (92.70)	91.60 (94.00)	94.00 (93.80)

Table 1: Accuracy [%] on test (training) data.

### 6.3 Nonlinear MPC benchmark: ethylene oxidation

We consider data generated from an ethylene oxidation plant model [29], that is used as a nonlinear MPC benchmark in the Model Predictive Control Toolbox for MATLAB [30]. A dataset of 2000 samples is generated by numerically integrating the system of nonlinear ordinary differential equations of the plant model with high accuracy and collecting values every  $T_s = 5$  s. The model generating the data has 4 states (gas density, C2H4 concentration, C2H4O concentration, and temperature in the reactor), one output (C2H4O concentration), and two inputs (total volumetric feed flow rate, that can be manipulated, and C2H4 concentration of the feed, which is a measured disturbance). Half the dataset ( $N = 1000$  samples) is used to train a RNN with  $L_x = 3$ ,  $L_y = 1$ ,

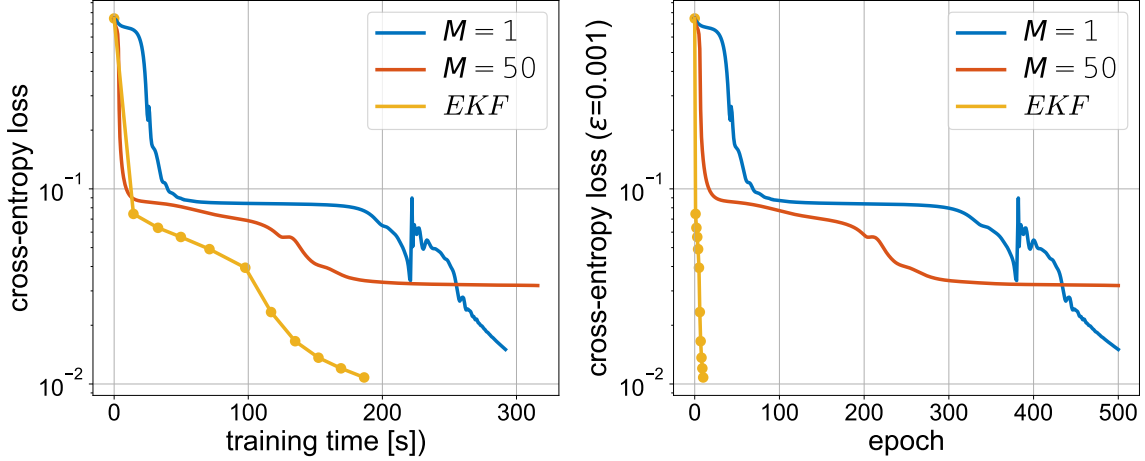


Figure 5: Linear system with binary outputs: cross-entropy training loss  $V(x_0, \theta)$  evaluated at each epoch

$n_x = n_1^x = n_2^x = 4$  (i.e., a two-layer state-update neural network), affine output function, sigmoidal activation functions  $f_1^x, f_2^x$ , and unit output function  $f_1^y$ . We run the EKF-based training algorithm by processing the dataset in  $N_e = 5$  epochs, which takes 126.68 s on the target machine. The NRMSE achieved by the learned RNN model is 94.18% on training data and 85.58% on test data.

After training the RNN model, we choose MPC weights  $W^{\Delta u} = 0.1$ ,  $W^y = 10$ ,  $u_{\min} = 0.0704$ ,  $u_{\max} = 0.7042$ , and prediction horizon  $p = 10$ . The corresponding NLMPC controller is implemented using PyTorch’s LBFGS solver with strong-Wolfe line-search method, 5 iteration maximum per optimization step, update history size of 100, and default tolerances, warm-started from the shifted previous optimal solution. As the solver does not support constrained optimization, the MPC performance index in (20) is augmented by the penalty on constraint violation  $10^3(\max\{u_t - u_{\max}, 0\}^2 + \max\{u_{\min} - u_t, 0\}^2)$  and the optimizer clipped within  $u_{\min}, u_{\max}$ .

To close the feedback loop and also guarantee offset-free tracking of constant set-points, the hidden state  $\hat{x}(k)$  is estimated by EKF applied on the extended RNN model (21) with  $B_d = 0$ ,  $C_d = 1$  (output disturbance model), that corresponds to only adapting the bias coefficient  $b_1^y$  in (1b), with covariances  $E[\xi(k)\xi(k)'] = 0.01I$ ,  $E[\eta(k)^2] = 1$ ,  $E[\zeta(k)^2] = 0.01$ , and  $P(0| -1) = I$ .

The obtained closed-loop results are depicted in Figure 6, where it is apparent that a very good tracking is achieved despite a black-box RNN model is used for prediction. The execution time employed by the Python code ranges between 56 ms and 472 ms (115 ms on average) to solve the NLMPC problem and between 1 ms and 4 ms (2 ms on average) for state estimation.

## 7 Conclusions

We have shown that EKF is an efficient way of learning RNN models from input and output data, both in an offline setting and online, even in the case of general strongly convex and twice-differentiable loss functions. The main limitation of the approach lies in the computation and manipulation of the Jacobian matrices of the state-update and output functions with respect to the parameters of the model, that limits the method to relatively small models, such as those typically used in nonlinear and adaptive model-based control.

Learning RNN models via EKF (offline or online) has the advantage that the covariance matrix

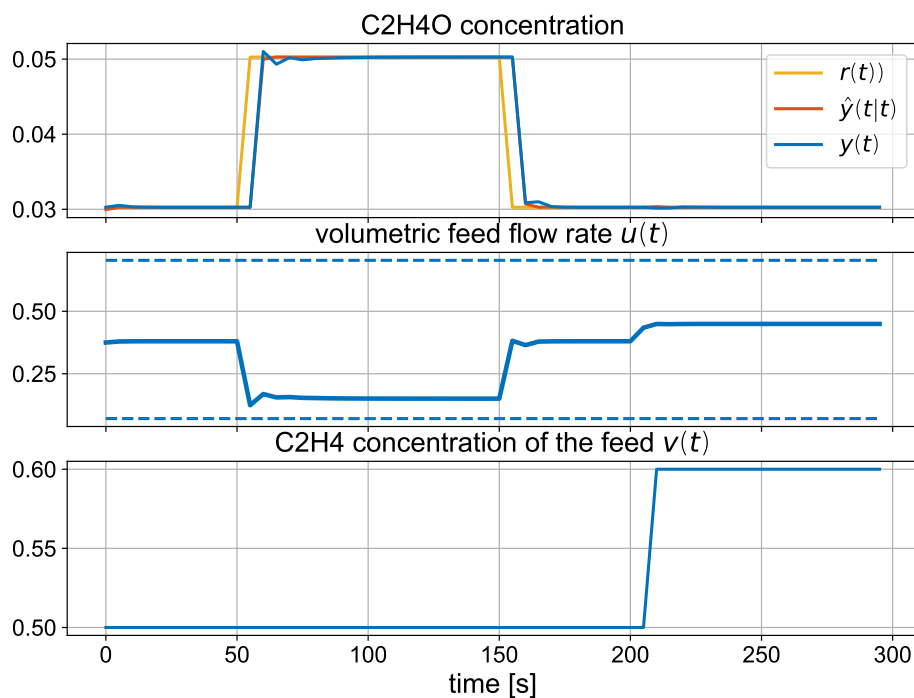


Figure 6: Ethilene oxidation benchmark: closed-loop NLMPC results

$P(k|k)$  directly quantifies the uncertainty associated with  $\theta$ . One could exploit this to setup robust or stochastic nonlinear MPC schemes. Another interesting feature of EKF-based learning is that it very naturally extends to gray-box identification of dynamical systems in which only some parts are modeled as black-box RNNs. An interesting topic for future research is to study the conditions to impose on the RNN structure to make  $x$  and  $\theta$  observable, in particular to prevent over-parameterizing the model.

## References

- [1] J. Suykens, J. Vandewalle, and B. D. Moor, *Artificial neural networks for modelling and control of non-linear systems*. Springer Science & Business Media, 1995.
- [2] V. Prasad and B. Bequette, “Nonlinear system identification and model reduction using artificial neural networks,” *Computers & chemical engineering*, vol. 27, no. 12, pp. 1741–1754, 2003.
- [3] D. Masti and A. Bemporad, “Learning nonlinear state-space models using autoencoders,” vol. 129, p. 109666, 2021.
- [4] R. Williams and J. Peng, “An efficient gradient-based algorithm for on-line training of recurrent network trajectories,” *Neural computation*, vol. 2, no. 4, pp. 490–501, 1990.
- [5] M. Forgione and D. Piga, “Model structures and fitting criteria for system identification with neural networks,” in *14th IEEE International Conference on Application of Information and Communication Technologies (AICT)*, Tashkent, Uzbekistan, 2020.

- [6] S. Singhal and L. Wu, "Training feed-forward networks with the extended Kalman algorithm," in *International Conference on Acoustics, Speech, and Signal Processing*, 1989, pp. 1187–1190.
- [7] G. Puskorius and L. Feldkamp, "Neurocontrol of nonlinear dynamical systems with Kalman filter trained recurrent networks," *IEEE Transactions on Neural Networks*, vol. 5, no. 2, pp. 279–297, 1994.
- [8] X. Wang and Y. Huang, "Convergence study in extended Kalman filter-based training of recurrent neural networks," *IEEE Transactions on Neural Networks*, vol. 22, no. 4, pp. 588–600, 2011.
- [9] R. Williams, "Training recurrent networks using the extended Kalman filter," in *IJCNN Int. Joint Conf. on Neural Networks*, vol. 4, 1992, pp. 241–246.
- [10] M. Matthews and G. Moschytz, "Neural network nonlinear adaptive filtering using the extended Kalman filtering algorithm," in *Proc. of the Int. Neural Networks Conf.*, Paris, France, 1990, pp. 115–119.
- [11] M. Livstone, J. Farrell, and W. Baker, "A computationally efficient algorithm for training recurrent connectionist networks," in *Proc. American Control Conference*, 1992, pp. 555–561.
- [12] D. Mirikitani and N. Nikolaev, "Efficient online recurrent connectionist learning with the ensemble Kalman filter," *Neurocomputing*, vol. 73, no. 4–6, pp. 1024–1030, 2010.
- [13] J. Nocedal and S. Wright, *Numerical Optimization*, 2nd ed. Springer, 2006.
- [14] P. J. Werbos, "Backpropagation through time: what it does and how to do it," *Proceedings of the IEEE*, vol. 78, no. 10, pp. 1550–1560, 1990.
- [15] S. Hochreiter, "Recurrent neural net learning and vanishing gradient," *International Journal Of Uncertainty, Fuzziness and Knowledge-Based Systems*, vol. 6, no. 2, pp. 107–116, 1998.
- [16] G. Hicks and W. Ray, "Approximation methods for optimal control synthesis," *The Canadian Journal of Chemical Engineering*, vol. 49, no. 4, pp. 522–528, 1971.
- [17] A. Bemporad and G. Cimini, "Reduction of the number of variables in parametric constrained least-squares problems," 2020, available on arXiv at <http://arxiv.org/abs/2012.10423>.
- [18] H. Bock and K.-J. Plitt, "A multiple shooting algorithm for direct solution of optimal control problems," *IFAC Proceedings Volumes*, vol. 17, no. 2, pp. 1603–1608, 1984.
- [19] D. Axehill, "Controlling the level of sparsity in MPC," *Systems & Control Letters*, vol. 76, pp. 1–7, 2015.
- [20] J. Humpherys, P. Redd, and J. West, "A fresh look at the Kalman filter," *SIAM Review*, vol. 54, no. 4, pp. 801–823, 2012.
- [21] B. Gibbs, *Advanced Kalman filtering, least-squares and modeling: a practical handbook*. John Wiley & Sons, 2011.



- [22] G. Pannocchia and J. Rawlings, “Disturbance models for offset-free MPC control,” *AIChE Journal*, vol. 49, no. 2, pp. 426–437, Feb. 2003.
- [23] G. Pannocchia, “Offset-free tracking MPC: A tutorial review and comparison of different formulations,” in *European Control Conference (ECC)*, Linz, Austria, 2015, pp. 527–532.
- [24] M. Vaccari, D. Bonvin, F. Pelagagge, and G. Pannocchia, “Offset-free economic MPC based on modifier adaptation: Investigation of several gradient-estimation techniques,” *Processes*, vol. 9, no. 5, p. 901, 2021.
- [25] A. Paszke et al., “PyTorch: An imperative style, high-performance deep learning library,” *Advances in neural information processing systems*, vol. 32, pp. 8026–8037, 2019, <https://pytorch.org/>.
- [26] S. Reddi, S. Kale, and S. Kumar, “On the convergence of adam and beyond,” *arXiv preprint arXiv:1904.09237*, 2019.
- [27] J. Wang, A. Sano, T. Chen, and B. Huang, “Identification of Hammerstein systems without explicit parameterisation of non-linearity,” *International Journal of Control*, vol. 82, no. 5, pp. 937–952, 2009.
- [28] L. Ljung, *System Identification Toolbox for MATLAB*. The Mathworks, Inc., <https://www.mathworks.com/help/ident>.
- [29] H. Durand, M. Ellis, and P. Christofides, “Economic model predictive control designs for input rate-of-change constraint handling and guaranteed economic performance,” *Computers & Chemical Engineering*, vol. 92, pp. 18–36, 2016.
- [30] A. Bemporad, M. Morari, and N. Ricker, *Model Predictive Control Toolbox for MATLAB*. The Mathworks, Inc., <http://www.mathworks.com/help/mpc>.